Sveriges lantbruksuniversitet
Swedish University of Agricultural Sciences

This is the peer reviewed version of the following article:

[1] # Estimating density from presence/absence data in clustered populations

[2]

[3] M. Ekström[a,b,1], S. Sandring[b], A. Grafström[b], P.-A. Esseen[c], B. G. Jonsson[d], G.

[4] Ståhl[b]

[5] [a] Department of Statistics, USBE, Umeå University, SE-901 87 Umeå, Sweden

[6] [b] Department of Forest Resource Management, Swedish University of Agricultural Sciences, SE-901 83 Umeå,

[7] Sweden

[8] [c] Department of Ecology and Environmental Science, Umeå University, SE-901 87 Umeå, Sweden

[9] [d] Department of Natural Sciences, Mid Sweden University, SE-851 70 Sundsvall, Sweden

[10]

[11] ## Summary

[12] 1. Inventories of plant populations are fundamental in ecological research and
[13] monitoring, but such surveys are often prone to field assessment errors. Pres-
[14] ence/absence (P/A) sampling may have advantages over plant cover assess-
[15] ments for reducing such errors. However, the linking between P/A data and
[16] plant density depends on model assumptions for plant spatial distributions.
[17] Previous studies have shown how that plant density can be estimated under
[18] e.g. Poisson model assumptions on the plant locations. In this study new
[19] methods are developed and evaluated for linking P/A data with plant density
[20] assuming that plants occur in clustered spatial patterns.

[21] 2. New theory was derived for estimating plant density under Neyman-Scott type
[22] cluster models such as the Matérn and Thomas cluster processes. Suggested
[23] estimators, corresponding confidence intervals, and a proposed goodness of fit
[24] test were evaluated in a Monte-Carlo simulation study assuming a Matérn
[25] cluster process. Further, the estimators were applied to plant data from envi-
[26] ronmental monitoring in Sweden to demonstrate their empirical application.

[27] 3. The simulation study showed that our methods work well for large enough
[28] sample sizes. The judgment of what is "large enough" is often difficult, but

[1] Corresponding author. *Email address*: Magnus.Ekstrom@umu.se (M. Ekström)

29 simulations indicate that a sample size is large enough when the sampling dis-

30 tributions of the parameter estimators are symmetric or mildly skewed. Boot-

31 strap may me used to check whether this is true. The empirical results suggests

32 that the derived methodology may be useful for estimating density of plants

33 such as *Leucanthemum vulgare* and *Scorzonera humilis*.

34 4. By developing estimators of plant density from P/A data under realistic model

35 assumptions about plants' spatial distributions, P/A sampling will become a

36 more useful tool for inventories of plant populations. Our new theory is an

37 important step in this direction.

38 **Key-words**: independent cluster process, intensity, Matérn cluster process, plant

39 monitoring, point pattern, sample plots, spatial models, Thomas cluster process,

40 vegetation survey

1 | INTRODUCTION

42 Inventories of plant communities are known to pose several challenges (Bonham

43 2013). Although broad-scale surveys of vegetation patterns may be based on remote

44 sensing data (Groom, Mücher, Ihse, & Wrbka, 2006), more detailed information

45 about species occurrences, vegetation cover, or plant densities rely on data from field-

46 based inventories. A common approach is to assess vegetation cover by species or

47 species groups on plots through visual inspection (Bråkenhielm & Liu, 1995; Bonham,

48 2013). However, this method is prone to surveyor judgment and the variability

49 among surveyors in assessing vegetation cover on a plot may be substantial (Gallegos-

50 Torell & Glimskär, 2009; Morrison, 2016). Presence/absence (P/A) sampling is

51 an alternative where only the presence or absence of a set of species on a plot is

52 registered. This sampling method is less prone to surveyor judgment than cover

53 assessments (Kercher, Frieswyk, & Zedler, 2003; Ringvall, Petersson, Ståhl, & Lämås,

54 2005; Milberg et al., 2008).

55 Normal outputs from inventories of plant communities include the abundance

2

of species in terms of plant density, cover, or biomass (Bonham, 2013). In P/A sampling, occurrence proportions are obtained, but such proportions are difficult to interpret since they depend on the used plot sizes (Ståhl et al., 2017). To obtain more easily interpreted outputs from P/A inventories, results need to re-expressed in terms of e.g. plant density. Such outputs need to be based on model assumptions regarding the spatial distribution of plants.

A commonly adopted assumption is that plant locations follow a homogeneous Poisson point process (HPPP) model (Bonham, 2013). This model possesses the property of complete spatial randomness, meaning that the events of a pattern are equally likely to occur anywhere and do not interact with each other. With such a model, recalculations from occurrence proportion to plant density is fairly straight-forward (Fisher, 1934; Bartlett, 1935; Ståhl et al., 2017). It should be noted that if the positions of plants follow a HPPP, they show neither positive spatial dependence (clustering) nor negative spatial dependence (regularity). The HPPP assumption is therefore seldom satisfied because plants are typically aggregated into clusters of different size and distribution across the landscape (Bonham, 2013; Ståhl et al., 2017). The closely related binomial point process arises from the HPPP by conditioning on the total number of plants in an area of interest. Arrhenius (1921) considers P/A data under such a model, and Royle & Nichols (2003) and He & Reed (2006) show how recalculations from occurrence proportion to plant density can be made.

The HPPP implies that the species abundance in a plot follows a Poisson distribution, while the binomial point process implies that it follows a binomial distribution. Another popular model for plot abundance is the negative binomial distribution, which is regarded useful in applications where a clustering alternative is preferred to the HPPP (He & Gaston, 2000, 2007; Hwang & He, 2011). However, only two known homogeneous point processes give the negative binomial distribution for plot abundances, and both are extreme cases (Daley & Vere-Jones, 2008). This highlights the need for more elaborate and realistic models for linking P/A data with plant density in clustered populations.

Although we recognize the possibility of using inhomogeneous models, where the

expected number of plants per area unit is spatially varying, we restrict the discussion in this paper to homogeneous models. We refer to, e.g., Baddeley, Rubak, & Turner (2016) and the references therein for a discussion on inhomogeneous Poisson process models and Gelfand & Shirota (2018) for fusion of P/A data with presence-only data using inhomogeneous log-Gaussian Cox processes.

Our objective was to represent a set of locations of plants in a landscape as a point pattern generated by general Neyman-Scott type cluster models, and to propose and evaluate a method for estimating the parameters in the assigned point process model, using data from P/A sampling. A particular objective was to derive an estimator of the intensity of the process (expected number of plants per area unit), and evaluate this estimator using both Monte Carlo simulations and empirical data from environmental monitoring. The intensity of a point process will henceforth be called the plant density, or simply density.

2 | MATERIAL AND METHODS

2.1 | Theoretical background

A clustered pattern can be constructed from a mechanism where "offspring" points are scattered around their respective "parent" points, e.g. young plants cluster around parent plants, where the offsprings arise from seeds or clonal growth (ramets) from the parent plant. To formalize the above, let X be a finite point process on $\mathbb{R}^2$. Conditioned on X, let Y_x be a finite point process centered at $x \in X$. If the processes Y_x, $x \in X$, are independent of one another given X, then $Y = \bigcup_{x \in X} Y_x$ is known as an *independent cluster process* (e.g. Lawson & Denison, 2002). The data consist of a realization of $Z = Y \cap S$, where $S \subset \mathbb{R}^2$ is a compact set.

Assumption P: The (parent) process X is a HPPP with density τ and the number of (offspring) points in Y_x is Poisson distributed, with mean λ. The points in Y_x are independently generated from $f(t - x|\gamma)$, where f is the density function of a

4

113 continuous random variable in $\mathbb{R}^2$ parameterized by γ.

114

115 Under Assumption P, the process $Y = \bigcup_{x \in X} Y_x$ is of Neyman-Scott type (Lawson
116 & Denison, 2002; Baddeley, Rubak, & Turner, 2016). Its density is $\tau\lambda$. By specifying
117 the offspring probability density $f(t - x|\gamma)$ in Assumption P, some well-known point
118 process models of clustering are obtained:

119 • If $f(t - x|\gamma)$ in Assumption P is a uniform density in a disc of radius γ centered
120   around the parent x, then the point process is a *Matérn cluster process* (Matérn,
121   1960, 1986). See Fig. 1.

122 • If $f(t - x|\gamma)$ in Assumption P is an isotropic bivariate normal density centered
123   around the parent x, with variance γ in the "x" and "y" directions, then the
124   point process is a (modified) *Thomas cluster process* (Thomas, 1949; Diggle,
125   1978).

126 Baddeley, Rubak, & Turner (2016) provide additional examples of point processes
127 that satisfy Assumption P, such as the Cauchy cluster process and the variance-
128 gamma cluster process.

129 The parameter vector $\boldsymbol{\theta} = (\tau, \lambda, \gamma)$ is unknown and needs to be estimated from
130 observed data. In the current paper we will derive estimators of $\boldsymbol{\theta}$ using P/A data
131 from sample plots. Let $N(B)$ denote the number of points that fall in $B \subseteq S$, i.e.,
132 $N(B) = \{z : z \in Z \cap B\}$. Note, $\{N(B) > 0\}$ is the event that at least one point is
133 present in B, and $\{N(B) = 0\}$ denotes absence of points in B.

134 Let

$$135 \quad H(B|\boldsymbol{\theta}) = \exp\left(-\tau \int \left(1 - \exp\left(-\lambda \int_B f(t - x|\gamma)dt\right)\right) dx\right), \quad B \subseteq S. \quad (1)$$

136 For deriving maximum likelihood estimators of $\boldsymbol{\theta}$ under Assumption P and various
137 sample plot designs, the following theorem is of fundamental importance. Among
138 other things, the theorem establishes that $H(B|\boldsymbol{\theta})$ is the probability of absence
139 of points in $B \subseteq S$, given that Assumption P holds true. More generally, given
140 disjoints sets $B_1, ..., B_m$, the theorem gives a formula for the probability of absence

of points in e.g. the first few of these sets and presence in the remaining ones. The theorem is essential for defining the likelihood function, which is used after data are available to describe plausibility of a parameter vector $\boldsymbol{\theta}$. Any parameter vector that maximizes the likelihood function (or, equivalently, its logarithm) is known as a maximum likelihood estimator, and intuitively it is the value of $\boldsymbol{\theta}$ that make the observed data most probable.

Theorem 1. *Let B_i, $i \in M = \{1, ..., m\}$, be disjoints sets in S, $M_s \subseteq M$, and $M_s^c = M \setminus M_s$. If Assumption P is valid, then*

$$P\{N(B_i) > 0, i \in M_s, \text{ and } N(B_i) = 0, i \in M_s^c\}$$

$$= H\left(\bigcup_{i \in M_s^c} B_i | \boldsymbol{\theta}\right) - \sum_{i \in M_s} H\left(B_i \cup \left[\bigcup_{j \in M_s^c} B_j\right] | \boldsymbol{\theta}\right)$$

$$+ \sum_{i_1, i_2 \in M_s, i_1 < i_2} H\left(B_{i_1} \cup B_{i_2} \cup \left[\bigcup_{j \in M_s^c} B_j\right] | \boldsymbol{\theta}\right) - ... + (-1)^{m_s} H\left(\bigcup_{i \in M} B_i | \boldsymbol{\theta}\right),$$

where m_s is the number of elements in the set M_s.

The proof of Theorem 1 is given in Appendix S1, Supporting Information. Usage of Theorem 1 is illustrated in the next two examples.

Example 1. Consider a concentric plot design, in which the jth innermost circle C_j has a radius r_j, $j = 1, ..., k$ (Fig. 2). Let $B_1 = C_1$ and $B_j = C_j \setminus C_{j-1}$, $j = 2, ..., k$. We assume that the surveyer starts with the innermost circle and move outwards, until the first plant (point) is observed. Thus, if no plants are present in $B_1, ..., B_{j-1}$, and at least one plant is present in B_j, where $j \leq k$, or if no plants are present in $C_k = \cup_{j=1}^k B_j$, then the surveyer is done, and moves on to the next set of concentric circular plots. Thus, we observe whether the following events are true or false,

$$A_0 = \{\text{absence in } C_k\} = \{N(C_k) = 0\},$$

$$A_1 = \{\text{presence in } C_1\} = \{N(C_1) > 0\},$$

$$A_j = \{\text{presence in } B_j \text{ but not in } C_{j-1}\} = \{N(C_{j-1}) = 0 \text{ and } N(B_j) > 0\}.$$

6

The corresponding probabilities are obtained from Theorem 1,

$$\pi_0 = P\{A_0\} = H(C_k|\boldsymbol{\theta}),$$

$$\pi_1 = P\{A_1\} = 1 - H(C_1|\boldsymbol{\theta}),$$

$$\pi_j = P\{A_j\} = H(C_{j-1}|\boldsymbol{\theta}) - H(C_j|\boldsymbol{\theta}), \quad j = 2, ..., k.$$

Example 2. In this example we consider a sample plot design used for monitoring of biodiversity in Sweden. For a list of plant species, P/A is recorded in subplots grouped into sets of nine 0.25 m^2 circular plots (Fig. 3). With such a subplot layout, C_j, $j = 1, ..., 9$, we define $B_0 = C_1 \cup C_2 \cup C_3$, $B_1 = C_4 \cup C_5$, $B_2 = C_6 \cup C_7$, and $B_3 = C_8 \cup C_9$. To reduce complexity we consider events defined using the B_i's rather than the C_j's. For notational convenience, let $B_{j:k} = \cup_{i=j}^k B_i$. The events that we consider are

$$A_0 = \{\text{absence in } B_{0:3}\},$$

$$A_1 = \{\text{presence in } B_0 \text{ but not in } B_{1:3}\},$$

$$A_2 = \{\text{absence in } B_0 \text{ and presence in exactly one of } B_1, B_2, \text{ and } B_3\},$$

$$A_3 = \{\text{presence in } B_0 \text{ and presence in exactly one of } B_1, B_2, \text{ and } B_3\},$$

$$A_4 = \{\text{absence in } B_0 \text{ and presence in exactly two of } B_1, B_2, \text{ and } B_3\},$$

$$A_5 = \{\text{presence in } B_0 \text{ and presence in exactly two of } B_1, B_2, \text{ and } B_3\},$$

$$A_6 = \{\text{absence in } B_0 \text{ and presence in each of } B_1, B_2, \text{ and } B_3\},$$

$$A_7 = \{\text{presence in each of } B_0, B_1, B_2, \text{ and } B_3\}.$$

The corresponding probabilities, $\pi_j = P\{A_j\}$, $j = 0, ..., 7$, are obtained using Theo-

rem 1 and the fact that the process is invariant under rotations and reflections,

$$\pi_0 = P\{N(B_{0:3}) = 0\} = H(B_{0:3}|\boldsymbol{\theta}),$$

$$\pi_1 = P\{N(B_{1:3}) = 0 \text{ and } N(B_0) > 0\} = H(B_{1:3}|\boldsymbol{\theta}) - H(B_{0:3}|\boldsymbol{\theta}),$$

$$\pi_2 = 3P\{N(B_{0:2}) = 0 \text{ and } N(B_3) > 0\} = 3(H(B_{0:2}|\boldsymbol{\theta}) - H(B_{0:3}|\boldsymbol{\theta})),$$

$$\pi_3 = 3P\{N(B_{2:3}) = 0, N(B_0) > 0, \text{ and } N(B_1) > 0\}$$

$$= 3(H(B_{2:3}|\boldsymbol{\theta}) - H(B_{0:2}|\boldsymbol{\theta}) - H(B_{1:3}|\boldsymbol{\theta}) + H(B_{0:3}|\boldsymbol{\theta})),$$

$$\pi_4 = 3P\{N(B_{0:1}) = 0, N(B_2) > 0, \text{ and } N(B_3) > 0\}$$

$$= 3(H(B_{0:1}|\boldsymbol{\theta}) - 2H(B_{0:2}|\boldsymbol{\theta}) + H(B_{0:3}|\boldsymbol{\theta})),$$

$$\pi_5 = 3P\{N(B_3) = 0, N(B_0) > 0, N(B_1) > 0, \text{ and } N(B_2) > 0\}$$

$$= 3(H(B_3|\boldsymbol{\theta}) - 2H(B_{2:3}|\boldsymbol{\theta}) - H(B_{0:1}|\boldsymbol{\theta}) + H(B_{1:3}|\boldsymbol{\theta}) + 2H(B_{0:2}|\boldsymbol{\theta}) - H(B_{0:3}|\boldsymbol{\theta})),$$

$$\pi_6 = P\{N(B_0) = 0, N(B_1) > 0, N(B_2) > 0, \text{ and } N(B_3) > 0\}$$

$$= H(B_0|\boldsymbol{\theta}) - 3H(B_{1:2}|\boldsymbol{\theta}) + 3H(B_{0:2}|\boldsymbol{\theta}) - H(B_{0:3}|\boldsymbol{\theta}),$$

$$\pi_7 = P\{N(B_0) > 0, N(B_1) > 0, N(B_2) > 0, \text{ and } N(B_3) > 0\} = 1 - \sum_{j=0}^{6} \pi_j.$$

2.2 | Estimation and hypothesis testing

The basis for our study is to link P/A registrations with plant density through Neyman-Scott type cluster models of plant occurrence. More specifically, focus will be on data collected according to the sample plot designs described in Examples 1 and 2, but our methodology can also be applied to many other sample plot designs.

In Example 1, assume that there are n sets of concentric circular plots, C_{ij}, $i = 1, ..., n$, $j = 1, ..., k$, or, in Example 2, assume that there are n sets of circular subplots, C_{ij}, $i = 1, ..., n$, $j = 1, ..., k$, where $k = 9$. Suppose that the $C_{i\bullet} = \cup_{j=1}^{k} C_{ij}$, $i = 1, ..., n$, are so far apart that it is not unreasonable to assume that the point patterns $Z_{i'} = Y \cap C_{i'\bullet}$ and $Z_{i''} = Y \cap C_{i''\bullet}$ are independent for all $i' \neq i''$. Let I_{ij} be the indicator of the event A_{ij}, $i = 1, ..., n$, $j = 0, ..., m$, where $m = k$ in Example 1 and $m = 7$ in Example 2. Note that $\pi_j = \pi_j(\boldsymbol{\theta})$, $j = 0, ..., m$, may be regarded as the probabilities in the $m+1$ cells of a multinomial distribution, and that $n_j = \sum_{i=1}^{n} I_{ij}$, $j = 0, ..., m$, are the observed frequencies in these cells.

8

Denote the true value of $\boldsymbol{\theta}$ by $\boldsymbol{\theta}_0$. The objective is to estimate $\boldsymbol{\theta}_0$ on the basis of the observed frequencies, n_j, $j = 0, ..., m$. Under Assumption P, the log-likelihood function for this problem is proportional to

$$l(\boldsymbol{\theta}) = \sum_{j=0}^{m} n_j \log \pi_j(\boldsymbol{\theta}), \tag{2}$$

and the maximum likelihood estimator of $\boldsymbol{\theta}_0$, denoted $\hat{\boldsymbol{\theta}} = (\hat{\tau}, \hat{\lambda}, \hat{\gamma})$, is defined as a $\boldsymbol{\theta}$-value in $\Theta = \{\boldsymbol{\theta} = (\tau, \lambda, \gamma) : \tau, \lambda, \gamma > 0\}$ that maximizes $l(\boldsymbol{\theta})$. Sufficient conditions under which the maximum likelihood estimator $\hat{\boldsymbol{\theta}}$ is consistent and asymptotically normally distributed are given in Rao (1973, Section 5e.2). It should be noted, however, that these conditions may be violated if $H(B|\boldsymbol{\theta})$ in (1) is not smooth enough as a function of γ; see Rao (1973) for details. For example, for asymptotic normality, $H(B|\boldsymbol{\theta})$ is not smooth enough if it fails to have first-order partial derivatives which are continuous at $\boldsymbol{\theta}_0$.

The maximum likelihood estimator of the density of the process is $\hat{\tau}\hat{\lambda}$, and for constructing a confidence interval for the density we argue as follows. Assuming that the information matrix $I(\boldsymbol{\theta}) = (i_{rs}(\boldsymbol{\theta}))$, given by

$$i_{rs}(\boldsymbol{\theta}) = \sum_{j=0}^{m} \frac{1}{\pi_j(\boldsymbol{\theta})} \frac{\partial \pi_j(\boldsymbol{\theta})}{\partial \theta_r} \frac{\partial \pi_j(\boldsymbol{\theta})}{\partial \theta_s}$$

where $\theta_1 = \tau$, $\theta_2 = \lambda$, and $\theta_3 = \gamma$, is non-singular at $\boldsymbol{\theta}_0 = (\tau_0, \lambda_0, \gamma_0)$, let $i^{rs}(\boldsymbol{\theta}_0)$, $r, s = 1, 2, 3$, denote the elements of the inverse to the matrix $I(\boldsymbol{\theta}_0)$. By the asymptotic normality of $\hat{\boldsymbol{\theta}}$, i.e., that

$$\sqrt{n}(\hat{\boldsymbol{\theta}} - \boldsymbol{\theta}_0) \xrightarrow{D} N(0, [I(\boldsymbol{\theta}_0)]^{-1}),$$

and the delta method (e.g. Lehmann, 1999), we have

$$\sqrt{n} \left(\log \hat{\tau} + \log \hat{\lambda} - \log \tau_0 - \log \lambda_0 \right) \xrightarrow{D} N \left(0, \frac{i^{11}(\boldsymbol{\theta}_0)}{\tau_0^2} + \frac{i^{22}(\boldsymbol{\theta}_0)}{\lambda_0^2} + \frac{2i^{12}(\boldsymbol{\theta}_0)}{\tau_0 \lambda_0} \right),$$

and this result together with yet another application of the delta method yield

$$\sqrt{n} \left(\hat{\tau}\hat{\lambda} - \tau_0 \lambda_0 \right) \xrightarrow{D} N \left(0, i^{11}(\boldsymbol{\theta}_0)\lambda_0^2 + i^{22}(\boldsymbol{\theta}_0)\tau_0^2 + 2i^{12}(\boldsymbol{\theta}_0)\tau_0 \lambda_0 \right).$$

9

Thus, an approximate 95% confidence interval for the density $\tau_0 \lambda_0$ of the cluster process is given by

$$\hat{\tau}\hat{\lambda} \pm 1.96 \sqrt{\frac{i^{11}(\hat{\boldsymbol{\theta}})\hat{\lambda}^2 + i^{22}(\hat{\boldsymbol{\theta}})\hat{\tau}^2 + 2i^{12}(\hat{\boldsymbol{\theta}})\hat{\tau}\hat{\lambda}}{n}}. \tag{3}$$

Corresponding approximate 95% confidence intervals for the individual parameters are given by

$$\hat{\theta}_r \pm 1.96 \sqrt{\frac{i^{rr}(\hat{\boldsymbol{\theta}})}{n}}, \quad r = 1, 2, 3, \tag{4}$$

where, again, $\theta_1 = \tau$, $\theta_2 = \lambda$, and $\theta_3 = \gamma$.

The above results assume that Assumption P is valid. For this reason it is of interest to assess whether or not our cluster model assumption holds true. For doing this, one may use the χ^2 goodness of fit statistic for a multinomial distribution (e.g. Bishop, Fienberg, & Holland 2007). The statistic is defined as

$$\chi^2 = n \sum_{j=0}^{m} \frac{(p_j - \hat{\pi}_j)^2}{\hat{\pi}_j} \tag{5}$$

where $p_j = n_j/n$ and $\hat{\pi}_j = \pi_j(\hat{\boldsymbol{\theta}})$. Under the null hypothesis that the cluster process model is valid, the statistic is asymptotically χ^2-distributed with $m - 3$ degrees of freedom (Bishop, Fienberg, & Holland 2007). If the statistic is improbably large according to that χ^2 distribution, then one rejects the null hypothesis.

2.3 | Computational issues

Analytic expressions for maximum likelihood estimators in complex models are usually not easily available, and numerical methods are needed for maximizing log-likelihood functions. In addition, numerical methods are needed for computing the $H(B|\boldsymbol{\theta})$ function in (1), on which the probabilities $\pi_j(\boldsymbol{\theta})$ and the likelihood functions are based. For the Thomas process, the inner integral in $H(B|\boldsymbol{\theta})$, i.e. $F_{\gamma,x}(B) = \int_B f(t - x|\gamma)dt$, may be computed using an efficient numerical method described in DiDonato & Jarnagin (1961), which is implemented in, for example, the `pmvnEll` function in the package `shotGroups` (Wollschlaeger, 2017) written

10

264 for use in R (R Core Team, 2019). If the point process is a Matérn cluster process,

265 $F_{\gamma,x}(B)$ may be computed analytically (Appendix S2).

266   For computing the outer integral in $H(B|\boldsymbol{\theta})$ we used the `polyCub.SV` function

267 in the R package `polyCub` (Meyer & Held, 2014, Supplement B), which is based

268 on the product Gauss cubature as proposed by Sommariva & Vianello (2007). In

269 `polyCub.SV`, the number of cubature points may be modified via the argument

270 nGQ. It defaults to 20. Increasing the number of points increases the accuracy of

271 the computation of the log-likelihood value but also increases the computation time.

272   In R, there are several numerical procedures for maximizing log-likelihood func-

273 tions. We used the general-purpose optimization routine `constrOptim`, which im-

274 plements, among others, the Nelder-Mead and the BFGS algorithms, and with which

275 one may maximize the log-likelihood subject to the constraints that $\tau, \lambda, \gamma > 0$. The

276 BFGS algorithm, which is a quasi-Newton method, uses both log-likelihood function

277 values and gradients to build up a picture of the three-dimensional surface to be

278 maximized, while the Nelder-Mead algorithm uses only values of the log-likelihood

279 function. We have tried both algorithms and found that BFGS is somewhat faster

280 and therefore preferred for computing estimates.

281 2.4 | Case examples

282 2.4.1 | A Monte Carlo study

283 Since the inner integral of $H(B|\boldsymbol{\theta})$ in (1) may be computed analytically for

284 the Matérn cluster process, we considered this particular process in our Monte

285 Carlo study. Realisations of the Matérn cluster process were generated with the

286 `rMatClust` algorithm in the `spatstat` package (Baddeley, Rubak, & Turner 2016)

287 and maximum likelihood estimates of $\boldsymbol{\theta}_0$ were obtained based on concentric plot de-

288 sign data with $r_j = 0.1$, $j = 1, ..., k$, and $k = 10$ (see Example 1).

289   In total, we studied eight different cases, where the cases refer to various parame-

290 ter setups. For each case, we generated 1000 replications of the process, and for each

291 such replication we computed the maximum likelihood estimate of $\boldsymbol{\theta}_0$ (Appendix S3),

performed the χ^2 goodness of fit test (5), and computed the confidence intervals (3) and (4). Based on the replicate estimates of $\boldsymbol{\theta}_0$, we estimated the median and the mean of the estimators of the individual parameters (τ, λ, and γ) and the density $\tau\lambda$ of the Matérn cluster process, for each case considered. Based on the same replicate estimates, we computed actual confidence levels (ACLs) and median lengths of the confidence intervals, as well as actual significance levels (ASLs) of the χ^2 goodness of fit test. In this study, the nominal confidence level and the nominal significance level were taken to be 95% and 5%, respectively.

2.4.2 | P/A data from environmental monitoring

The National Inventory of Landscapes (NILS) is a nation-wide environmental monitoring programme with 631 permanent sample units (5×5 km^2) that form a random systematic grid across Sweden (Esseen, Glimskär, Ståhl, & Sundquist 2007). The programme started in 2003 and includes field inventory (and aerial photo interpretation) of permanent sample plots in all types of terrestrial environments. Field sampling is conducted every fifth year in circular plots of different sizes depending on the measured parameters (Ståhl et al., 2011). NILS provides an infrastructure for other monitoring and research programmes that need basic landscape data. Data for this study were obtained from three monitoring projects associated with NILS. These projects use the same method of collecting P/A-data of plants in 9 subplots (Fig. 3), whereas the original NILS methodology only includes 3 subplots per plot.

The first part of the data was obtained from a monitoring programme on semi-natural grassland, pastures and meadows, where data were collected in randomly selected grasslands within NILS sample units that earlier have been identified in a national inventory (Jordbruksverket, 2005). The second part was obtained from monitoring of terrestrial habitats (MOTH) under the European Habitats Directive (Gardfjell, Hagner, Adler, & Forsman, unpubl.), and the third part from regional monitoring of grasslands and wetlands (Rygne, 2009). All data were collected during 2009-2013. From the combined data set only plots classified as pastures and grasslands were included. To minimize variation in conditions further, the sample

12

was restricted to strata 1-5 (Fig. 4), where most grassland plants have their main distribution in Sweden. Only subplots with a tree cover less than 50% were used. Finally, only plots with a complete set of P/A data for all nine subplots were included for analysis ($n = 2109$).

As in Ståhl et al. (2017), the theory assumes that plant occurrences on a subplot are registered whenever a predetermined reference point of a plant is located on the subplot. However, registrations of presences were made if any part of a plant was located on a subplot, and therefore we made a correction by adding a presumed average plant radius to each subplot radius in the calculations. The presumed radius of a plant was set to 10 cm, except for *Scorzonera humilis*, where it was set to 12 cm.

3 | RESULTS

3.1 | The Monte Carlo study

Following the setup of the Monte Carlo study of the concentric plot design for the Matérn cluster process described in Section 2.4.1, we studied eight different cases. In most cases (Cases 1 to 6), the estimators showed no or very little bias, except for the mean cluster size λ and the density $\tau\lambda$ of the Matérn cluster process, where the estimators tended to have a small upward mean-bias (Table 1). Also, in all these cases, the ACLs and ASLs were close or quite close to their respective nominal levels (Tables 1 and 2), and, as illustrated in Fig. 5 for Case 6, the estimators tended to be approximately normally distributed. The standard errors of the estimates of τ, λ, and γ and the median lengths of the corresponding confidence intervals increased with increasing values of the respective corresponding true parameters (Table 1).

In the last two cases (Cases 7 and 8), the density τ of the parent process and the cluster radius γ were relatively large, and the estimators of γ and $\tau\lambda$ showed only a small upward mean-bias (Table 1). The estimators of τ and λ were, however, more heavily mean-biased (and median-biased). In addition, the ACLs for λ and γ were

notably lower than the nominal level. The was noticed also for the ASLs (Table 2). In both Cases 7 and 8, the estimators had notably skewed distributions, except for the estimator of the density $\tau\lambda$ (the histograms in Fig. 6 illustrates this for Case 7). In comparison with Cases 1-6, the sample size n in Cases 7 and 8 needed to be larger before the asymptotic properties "kicked in." For these latter two cases, results for $n = 10,000$ are presented in Tables 3-4 and Fig. 7. The histograms for $\hat{\lambda}$ and $\hat{\gamma}$ for Case 7 (Fig. 7) still show some skewness and some of the estimators in Table 3 still have some small upward mean-biases, but in comparison with the corresponding results for $n = 2000$ (Tables 1-2 and Fig. 6) the results were much improved.

3.2 | P/A data from environmental monitoring

In Table 5, the empirical results based on monitoring data are presented for three different plant species. The p-value for the goodness of fit test of the Matérn cluster process assumption is given for each species. It can be observed that two of the species, *Leucanthemum vulgare* and *Scorzonera humilis*, passed the goodness of fit test. For the chi-square approximation to be valid, a common rule of thumb is that (estimated) expected frequencies, $n\hat{\pi}_i$, $i = 0, ..., 7$, should be at least 5. Therefore, when we performed the goodness of fit test for *L. vulgare* and *S. humilis*, category $i = 4$ was merged with $i = 6$ and category $i = 5$ with $i = 7$, and, for *Pimpinella saxifraga*, category $i = 4$ was merged with $i = 6$.

The Monte Carlo study in the previous subsection suggests that the proposed estimation method works well when the sampling distributions of the parameter estimators are symmetric or mildly skewed. To check whether this holds true or not for the *L. vulgare* data, we applied the bootstrap (e.g. Davison & Hinkley, 1997). That is, bootstrap samples of size n, with replacement, were drawn from the original sample of n sets of subplots, and estimates of parameters were computed for each bootstrap sample. The resulting histograms are shown in Fig. 8. The "bootstrap distributions" for the density of the parent process, the mean cluster size, and the density of the Matérn cluster process had only mild skewness, suggesting that the estimators $\hat{\tau}$, $\hat{\lambda}$, and $\widehat{\tau\lambda}$ are nearly unbiased. The same conclusion was drawn for *S.*

14

³⁷⁷ *humilis.*

4 | DISCUSSION

³⁷⁹ Elzinga, Salzer, & Willoughby (1998) argue that the key advantages of P/A
³⁸⁰ sampling are "that no special skills are required (anyone who can recognize the species
³⁸¹ can do the monitoring) and that the monitoring requires very little time." On the
³⁸² other hand, a significant drawback of the method is that it does not generally provide
³⁸³ information on plant density, although some authors have studied this problem under
³⁸⁴ simple point pattern models such as the HPPP model (e.g. Fisher, 1934; Ståhl et
³⁸⁵ al., 2017). In this study, we develop new theory for linking P/A data with plant
³⁸⁶ density, and extend previous work to Neyman-Scott type cluster models such as the
³⁸⁷ Matérn and Thomas cluster processes. For practical purposes, this is of importance,
³⁸⁸ since plants typically form clusters of varying scales of patterns across the landscape
³⁸⁹ (Bonham, 2013), which can not be modeled using HPPP models.

³⁹⁰ In addition to deriving a maximum likelihood estimator of plant density, we
³⁹¹ suggest a corresponding confidence interval for the plant density. Both the estimator
³⁹² and the confidence interval rely on model assumptions, and may fail when the model
³⁹³ is incorrect. For this reason we propose a χ^2 goodness of fit test for testing if
³⁹⁴ the P/A data fits the assigned cluster process model. A simulation study shows
³⁹⁵ that the suggested estimator, confidence interval, and test work well when using a
³⁹⁶ suitable plot design together with a large enough sample size n for various clustered
³⁹⁷ populations. Our simulations indicate that a sample size is large enough when the
³⁹⁸ sampling distributions of the parameter estimators are symmetric or mildly skewed.
³⁹⁹ To check whether this holds true or not in a practical application, bootstrap may be
⁴⁰⁰ used to estimate the sampling distributions (e.g. Davison & Hinkley, 1997).

⁴⁰¹ Although the proposed approach for estimating plant density may be imple-
⁴⁰² mented for a large range of species, we recognize that this may imply significant
⁴⁰³ analytical work. Hence, we believe that a good starting point is to focus on a few
⁴⁰⁴ focal species, such as invasive species or threatened species. For these, the popula-

<div align="center">15</div>

tion size (density) is of particular interest to estimate and follow. We recommend using a Matérn cluster model initially, unless the nature of the data clearly suggests another choice. The main reason is that its implementation requires less numerical integration than for other Neyman-Scott type cluster models.

The impact of deviations from the model assumptions is an important topic for further studies, as well as extensions to inhomogeneous cluster point processes that allow the density of the process to be location dependent. The latter may be obtained by allowing model parameters to depend on covariate information. Of particular interest here are the cleverly constructed inhomogeneous Neyman-Scott processes in Waagepetersen (2007), with special cases such as the inhomogeneous Matérn and Thomas cluster processes (Baddeley, Rubak, & Turner, 2016). Stratified approaches may also be used. Here the strata may be those defined in the sampling design, or post-strata based on land use or land cover categories, or more advanced schemes employing several sources of information available wall-to-wall for the study area (e.g. Saarela et al., 2015).

Another important topic for further studies is to explore different P/A sampling designs and to find designs and plot sizes that will yield estimators of plant density with as high precision as possible, given that the design is cost-efficient, reliable, and good enough for practical purposes. For example, a plot design with relatively small plot sizes suitable for one species may not be appropriate for another species with different density. Both theoretical and empirical studies in this direction are needed. A promising candidate for P/A sampling that enables modeling of cluster point processes is the concentric plot design discussed in this paper. Another appealing possibility is P/A sampling of equally sized quadratic field plots, grouped into sets of 2×2 contiguous quadrats (cf. Morrison, Le Brocque, & Clarke, 1995).

| AUTHORS' CONTRIBUTIONS

M.E. conceived the idea, designed the analysis methodology, and conducted the analyses; G.S. contributed with expertise in field inventories and P/A sampling; S.S.

16

retrieved the data from projects integrated with the National Inventory of Landscapes (NILS) and contributed to the analysis with NILS knowledge; P.A.E. and B.G.J. contributed with the ecological perspectives underlying the analyses; A.G. contributed to the statistical methodology. All authors contributed to writing the article and the literature review. The final version of the article has been approved by all authors.

| ACKNOWLEDGEMENTS

| DATA ACCESSIBILITY

Upon acceptance of the paper, we intend to archive our empirical data at the Dryad Digital Repository.

| References

Arrhenius, O. (1921). Species and area. Journal of Ecology, 9, 95–99. doi: 10.2307/2255763

Baddeley, A., Rubak, E., & Turner, R. (2016). Spatial point patterns: Methodology and applications with R. Boca Raton, FL: CRC Press.

Bartlett, M.S. (1935) Appendix in Blackman, G.E. 1935. A study by statistical methods of the distribution of species in grassland associations. Annals of Botany, 49, 749–777. doi: 10.1093/oxfordjournals.aob.a090534

Bishop, Y. M., Fienberg, S. E., & Holland, P. W. (2007). Discrete multivariate analysis: Theory and practice. New York, NY: Springer Science & Business Media.

Bonham, C. D. (2013). Measurements for terrestrial vegetation (2nd ed.). New York, NY: John Wiley & Sons.

Bråkenhielm, S., & Liu, Q. (1995). Comparison of field methods in vegetation monitoring. Water, Air and Soil Pollution, 79, 75–87. doi: 10.1007/BF01100431

Daley, D. J., & Vere-Jones, D. (2008). An introduction to the theory of point processes (2nd ed.). New York, NY: Springer-Verlag.

Davison, A. C., & Hinkley, D. V. (1997). Bootstrap methods and their application. Cambridge: Cambridge University Press.

DiDonato, A. R., & Jarnagin, M. P. (1961). Integration of the general bivariate Gaussian distribution over an offset circle. Mathematics of Computation, 15, 375–382. doi: 10.1090/S0025-5718-1961-0129116-8

Diggle, P. J. (1978). On parameter estimation for spatial point processes. Journal of the Royal Statistical Society, Series B, 40, 178–181.

Elzinga, C. L., Salzer, D. W., & Willoughby, J. W. (1998). Measuring and monitoring plant populations. BLM Technical Reference 1730-1. BLM National Applied Resource Sciences Center. Denver, Colorado.

Esseen, P.-A., Glimskär, A., Ståhl, G., & Sundquist, S. (2007). Field instruction for the national inventory of the landscape in Sweden, NILS. Swedish University of Agricultural Sciences, Department of Forest Resource Management, Umeå, SE.

Fisher, R. A. (1934). Statistical Methods for research workers (5th ed.). Edinburgh: Oliver & Boyd.

Gallegos-Torell, Å., & Glimskär, A. (2009). Computer-aided calibration for visual estimation of vegetation cover. Journal of Vegetation Science, 20, 973–983. doi: 10.1111/j.1654-1103.2009.01111.x

Gardfjell, H., Hagner, Å., Adler, S., & Forsman, H. (unpublished). Habitat Inventory by Aerial Photo Interpretation in MOTH – Terrestrial and Seashore Inventory. www.slu.se/en/Collaborative-Centres-and-Projects/moth/.

Gelfand, A. E., & Shirota, S. (2018). Preferential sampling for presence/absence data and for fusion of presence/absence data with presence-only data. arXiv:1809.01322v1 [stat.ME].

Groom, G., Mücher, C. A., Ihse, M., & Wrbka, T. (2006). Remote sensing in landscape ecology: experiences and perspectives in a European context. Landscape Ecology, 21,

486   391–408. doi: 10.1007/s10980-004-4212-1

487   He, F., & Gaston, K. J. (2000) Estimating species abundance from occurrence. The Amer-
488   ican Naturalist, 156, 553–559. doi: 10.1086/303403

489   He, F., & Gaston, K. J. (2007). Estimating abundance from occurrence: an underdeter-
490   mined problem. The American Naturalist, 170, 655–659. doi: 10.1086/521340

491   He, F., & Reed, W. (2006). Downscaling abundance from the distribution of species:
492   occupancy theory and applications. In J. Wu, K. B. Jones, H. Li, & O. L. Loucks
493   (Eds.), *Scaling and uncertainty analysis in ecology: Methods and applications* (pp. 89–
494   108). Dordrecht: Springer.

495   Hwang, W.-H., & He, F. (2011). Estimating abundance from presence/absence maps.
496   Methods in Ecology and Evolution, 2, 550–559. doi: 10.1111/j.2041-210X.2011.00105.x

497   Jordbruksverket (2005). Ängs- och betesmarksinventeringen 2002-2004 [Result of the Sur-
498   vey of semi-natural pastures and meadows]. Jordbruksverket, Rapport 1, 44 p. (in
499   Swedish with English summary).

500   Kercher, S. M., Frieswyk, C. B., & Zedler, J. B. (2003). Effects of sampling teams and
501   estimation methods on the assessment of plant cover. Journal of Vegetation Science,
502   14, 899–906. doi: 10.1111/j.1654-1103.2003.tb02223.x

503   Lawson, A. B., & Denison, D. G. T., editors (2002). Spatial cluster modelling. Boca
504   Raton, FL: Chapman & Hall/CRC Press.

505   Lehmann, E. L. (1999). Elements of large-sample theory. New York, NY: Springer.

506   Matérn, B. (1960). Spatial variation: stochastic models and their application to some
507   problems in forest surveys and other sampling investigations. Meddelanden från Statens
508   Skogsforskningsinstitut, 49(5), 1–144.

509   Matérn, B. (1986). Spatial Variation. Lecture Notes in Statistics 36. New York, NY:
510   Springer Verlag.

511   Meyer, S., & Held, L. (2014). Power-law models for infectious disease spread. Annals of
512   Applied Statistics, 8, 1612–1639. doi: 10.1214/14-AOAS743

513   Milberg, P., Bergstedt, J., Fridman, J., Odell, G., & Westerberg, L. (2008). Observer bias
514   and random variation in vegetation monitoring data. Journal of Vegetation Science,
515   19, 633–644. doi: 10.3170/2008-8-18423

19

516 Morrison, L. W. (2016). Observer error in vegetation surveys: a review. Journal of Plant

517   Ecology 9, 367–379. doi: 10.1093/jpe/rtv077

518 Morrison, D. A., Le Brocque, A. F., & Clarke, P. J. (1995). An assessment of some

519   improved techniques for estimating the abundance (frequency) of sedentary organisms.

520   Vegetation, 120, 131–145. doi: 10.1007/BF00034343

521 Rao, C. R. (1957). Maximum likelihood estimation for multinomial distribution. Sankhyā,

522   18, 139–148.

523 Rao, C. R. (1973). Linear statistical inference and its applications. New York, NY: John

524   Wiley & Sons.

525 R Core Team (2019). R: A language and environment for statistical computing. R Foun-

526   dation for Statistical Computing, Vienna, Austria. URL https://www.R-project.org/.

527 Ringvall, A., Petersson, H., Ståhl, G., & Lämås, T. (2005). Surveyor consistency in P/A

528   sampling for monitoring vegetation in a boreal forest. Forest Ecology and Management,

529   212, 109–117. doi: 10.1016/j.foreco.2005.03.002

530 Royle, J. A., & Nichols, J. D. (2003). Estimating abundance from repeated presence-

531   absence data or point counts. Ecology, 84, 777–790. doi: 10.1890/0012-

532   9658(2003)084[0777:EAFRPA]2.0.CO;2

533 Rygne, H. (ed.) (2009). Metodutveckling för regional miljöövervakning och miljömål-

534   suppföljning via NILS. Länsstyrelsen i Örebro län, 2009:25 (in Swedish).

535 Saarela, S., Grafström, A., Ståhl, G., Kangas, A., Holopainen, M., Tuominen, S., ...

536   Hyyppä, J. (2015). Model-assisted estimation of growing stock volume using different

537   combinations of LiDAR and Landsat data as auxiliary information. Remote Sensing of

538   Environment, 158, 431–440. doi: 10.1016/j.rse.2014.11.020

539 Sommariva, A., & Vianello, M. (2007). Product Gauss cubature over polygons based

540   on Green's integration formula. BIT Numerical Mathematics, 47, 441–453. doi:

541   10.1007/s10543-007-0131-2

542 Ståhl, G., Allard, A., Esseen, P.-A., Glimskär, A., Ringvall, A., Svensson, J., ... Inghe, O.

543   (2011). National Inventory of Landscapes in Sweden (NILS) – scope, design, and expe-

544   riences from establishing a multiscale biodiversity monitoring system. Environmental

545   monitoring and assessment, 173, 579–595. doi: 10.1007/s10661-010-1406-7

546 Ståhl, G., Ekström, M., Dahlgren, J., Esseen, P.-A., Grafström, A., & Jonsson, B. G.

547   (2017). Informative plot sizes in presence-absence sampling of forest floor vegetation.

548   Methods in Ecology and Evolution, 8, 1284–1291. doi: 10.1111/2041-210X.12749

549 Thomas, M. (1949). A generalisation of Poisson's binomial limit for use in ecology.

550   Biometrika, 36, 18–25. doi: 10.2307/2332526

551 Waagepetersen, R. (2007). An estimating function approach to inference for inhomo-

552   geneous Neyman-Scott processes. Biometrics, 63, 252–258. doi: 10.1111/j.1541-

553   0420.2006.00667.x

554 Wollschlaeger, D. (2017). shotGroups: Analyze shot group data. R package version 0.7.3.

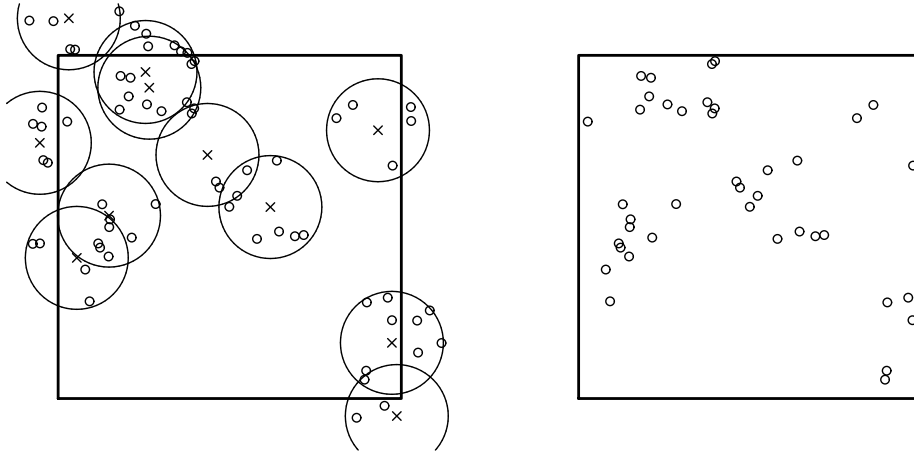555   https://CRAN.R-project.org/package=shotGroups

Fig. 1: A Matérn cluster process with parent density $\tau = 6$, mean cluster size $\lambda = 5$, and cluster radius $\gamma = 0.15$. The left panel shows parents (crosses), cluster regions (with radius γ), and offsprings (small open circles). The right panel shows the offsprings that constitute the Matérn cluster process in a square field S.
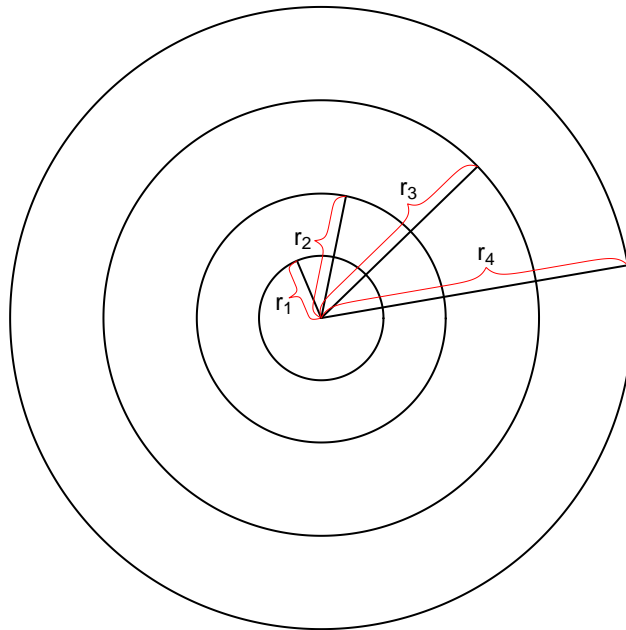

Fig. 2: Plot design with concentric circular sample plots with radii $r_1, ..., r_4$.
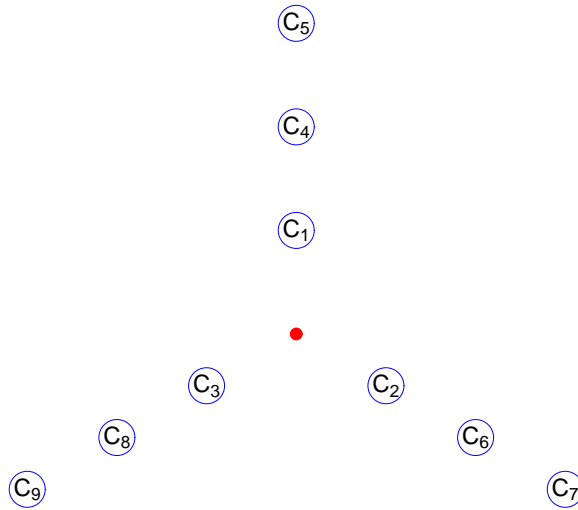
Fig. 3: Field subplot layout in Example 2. The distance from the centre (the red solid circle) to the centre of C_i, $i = 1, 2, 3$, is 3 m. The corresponding distances to C_i, $i = 4, 6, 8$, and to C_i, $i = 5, 7, 9$, are 5 and 7 m, respectively. The area of each C_i is 0.25 m^2.
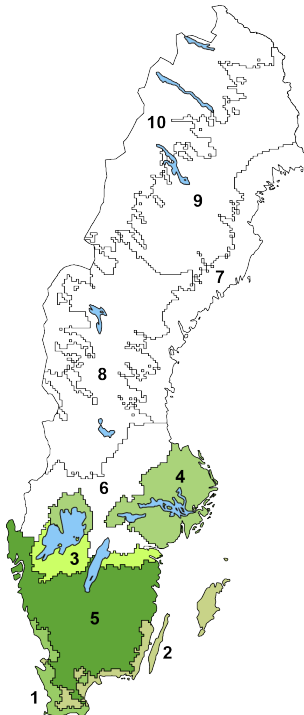

Fig. 4: Map of Sweden showing 10 strata used in NILS. Data from strata 1–5 were selected for the study.
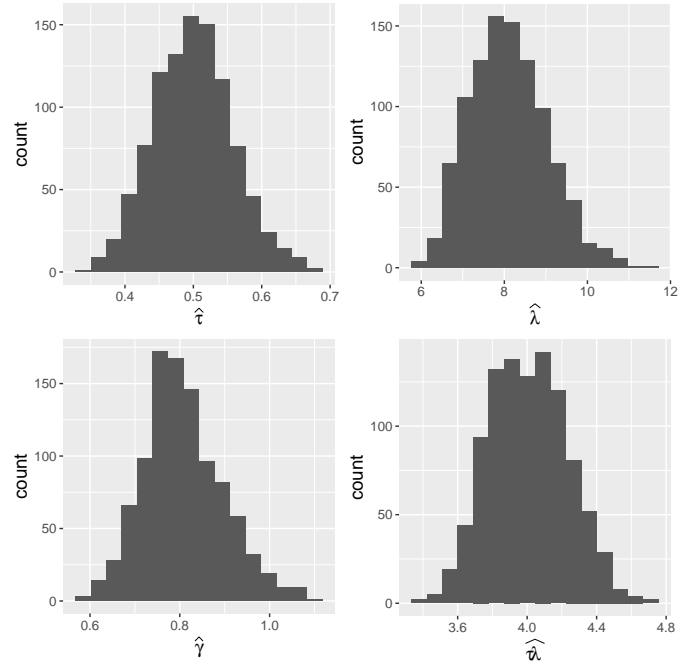
Fig. 5: Histograms of estimates: Case 6 with $n = 2000$.
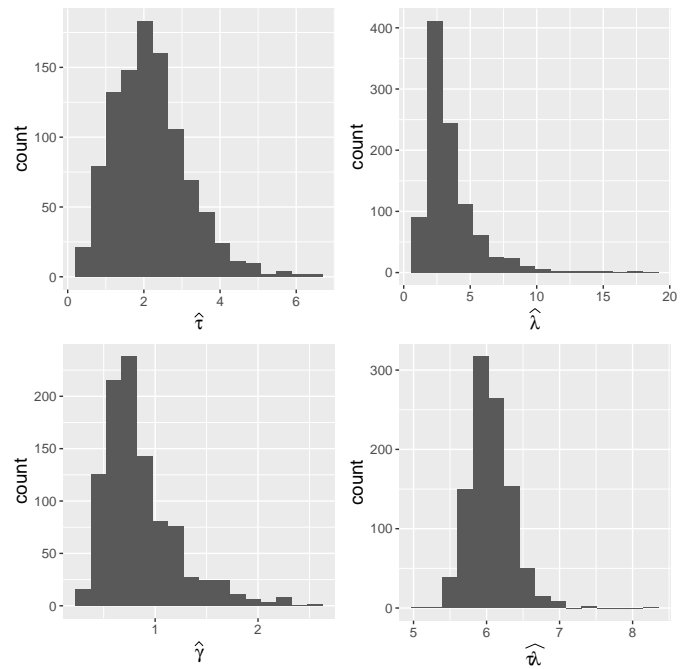

Fig. 6: Histograms of estimates: Case 7 with $n = 2000$.
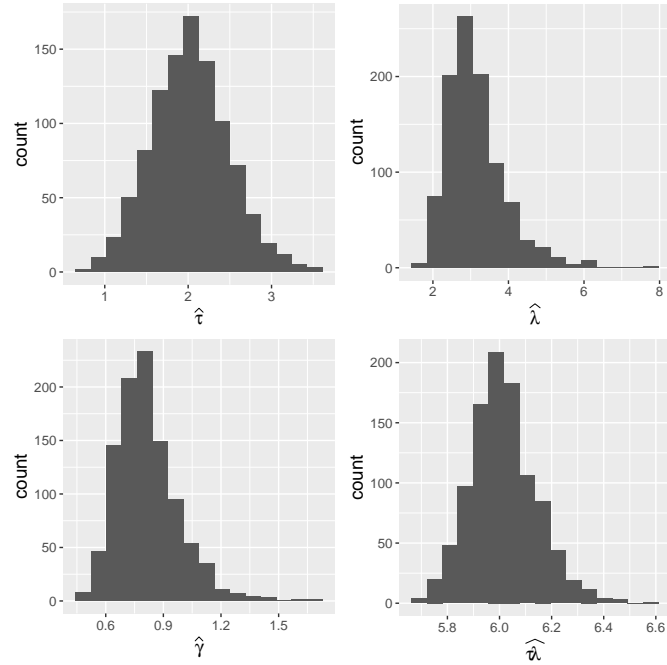
Fig. 7: Histograms of estimates: Case 7 with $n = 10,000$.
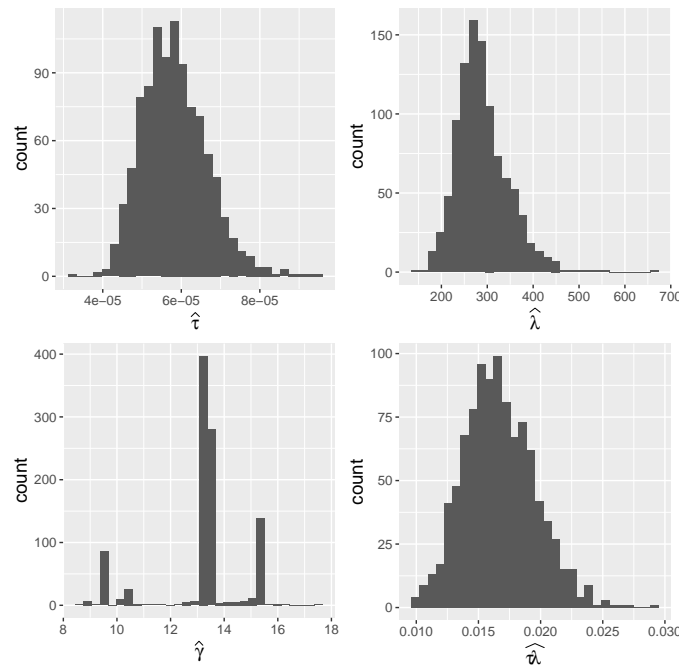

Fig. 8: Histograms of 1000 bootstrap replicates of estimates for the *Leucanthemum vulgare* data.

Table 1: Medians, means and standard errors (SEs) of estimates, and actual confidence levels (ACLs) and median lengths (MedLs) of the associated confidence intervals. The sample size is $n = 2000$.

	Parameter	True value	Median	Mean	SE	ACL (%)	MedL
	τ	0.50	0.50	0.50	0.04	96.2	0.13
Case 1	λ	3.00	3.01	3.12	0.71	95.8	2.35
	γ	0.30	0.30	0.31	0.08	96.2	0.26
	$\tau\lambda$	1.50	1.50	1.56	0.32	94.8	0.98
	τ	0.50	0.50	0.50	0.02	95.0	0.10
Case 2	λ	8.00	7.98	8.09	1.25	94.8	4.48
	γ	0.30	0.30	0.30	0.03	96.8	0.13
	$\tau\lambda$	4.00	3.98	4.06	0.63	94.1	2.24
	τ	2.00	1.99	2.00	0.16	96.2	0.62
Case 3	λ	3.00	3.05	3.05	0.35	96.5	1.42
	γ	0.30	0.30	0.30	0.05	95.5	0.18
	$\tau\lambda$	6.00	6.03	6.08	0.58	94.9	2.14
	τ	2.00	2.01	2.01	0.15	95.3	0.58
Case 4	λ	8.00	8.04	8.06	0.74	95.8	2.91
	γ	0.30	0.30	0.30	0.03	95.3	0.11
	$\tau\lambda$	16.00	16.03	16.17	1.43	95.5	5.22
	τ	0.50	0.50	0.50	0.07	96.2	0.28
Case 5	λ	3.00	3.04	3.11	0.51	97.2	1.70
	γ	0.80	0.80	0.82	0.17	95.2	0.56
	$\tau\lambda$	1.50	1.50	1.51	0.10	94.2	0.39
	τ	0.50	0.50	0.50	0.06	93.8	0.21
Case 6	λ	8.00	8.04	8.11	0.92	95.1	3.38
	γ	0.80	0.80	0.81	0.09	94.4	0.32
	$\tau\lambda$	4.00	4.00	4.01	0.23	95.5	0.88
	τ	2.00	2.09	2.18	0.98	93.6	3.82
Case 7[1]	λ	3.00	2.89	3.52	2.14	86.5	5.51
	γ	0.80	0.78	0.85	0.36	88.5	1.18
	$\tau\lambda$	6.00	6.02	6.05	0.29	96.1	1.10
	τ	2.00	2.17	2.44	1.43	94.9	4.64
Case 8	λ	8.00	7.36	8.56	4.68	86.2	15.43
	γ	0.80	0.76	0.84	0.83	88.3	1.09
	$\tau\lambda$	16.00	16.07	16.13	0.67	97.1	2.76

[1] The results shown are based on the 999 (out of 1000) replications that converged.

Table 2: Actual significance levels (ASLs) for the goodness of fit test of cases presented in Table 1. The sample size is $n = 2000$.

Case	ASL (%)
1	5.0
2	5.6
3	5.5
4	6.4
5	5.7
6	5.3
7[1]	3.9
8	2.8

[1] The results shown are based on the 999 (out of 1000) replications that converged.

Table 3: Medians, means and standard errors (SEs) of estimates, and actual confidence levels (ACLs) and median lengths (MedLs) of the associated confidence intervals. The sample size is $n = 10,000$.

	Parameter	True value	Median	Mean	SE	ACL (%)	MedL
	τ	2.00	2.01	2.02	0.47	93.6	1.78
Case 7	λ	3.00	3.00	3.15	0.80	92.3	2.62
	γ	0.80	0.79	0.82	0.16	92.8	0.56
	$\tau\lambda$	6.00	6.01	6.01	0.13	94.4	0.50
	τ	2.00	2.07	2.10	0.52	94.4	2.08
Case 8	λ	8.00	7.77	8.10	2.03	91.6	7.75
	γ	0.80	0.79	0.80	0.13	93.1	0.53
	$\tau\lambda$	16.00	16.00	16.02	0.31	95.2	1.21

Table 4: Actual significance levels (ASLs) for the goodness of fit test of cases presented in Table 3. The sample size is $n = 10,000$.

Case	ASL (%)
7	4.6
8	4.7

Table 5: Estimated parameters of the Matérn cluster process (the estimated density $\hat{\tau}$ of the parent process (parent plants per m^2), estimated mean cluster size $\hat{\lambda}$, estimated cluster radius $\hat{\gamma}$ (m), and estimated density $\widehat{\tau\lambda}$ of the Matérn cluster process (plants per m^2)) and the p-value of the goodness of fit test.

Species	$\hat{\tau}$	$\hat{\lambda}$	$\hat{\gamma}$	$\widehat{\tau\lambda}$	p-value
Leucanthemum vulgare (oxeye daisy)	0.000063	271.8	12.1	0.017	0.055
Pimpinella saxifraga (burnet-saxifrage)	0.000089	648.0	13.6	0.058	0.00013
Scorzonera humilis (viper's-grass)	0.0000054	1843.3	39.1	0.010	0.68